Characterizing an Image Intensifier in a Full-Field Range Imaging System

Andrew D. Payne, Adrian A. Dorrington, Michael J. Cree, *Senior Member, IEEE*, and Dale A. Carnegie, *Senior Member, IEEE*

***Abstract*—We are developing a high precision full-field range imaging system. An integral component in this system is an image intensifier, which is modulated at frequencies up to 100 MHz. The range measurement precision is dictated by the image intensifier performance, in particular, the achievable modulation frequency, modulation depth, and waveform shape. By characterizing the image intensifier response, undesirable effects can be observed and quantified with regards to the consequence on the resulting range measurements, and the optimal operating conditions can be selected to minimize these disturbances.**

The characterization process utilizes a pulsed laser source to temporally probe the gain of the image intensifier. The laser is pulsed at a repetition rate slightly different to the image intensifier modulation frequency, producing a continuous phase shift between the two signals. A charge coupled device samples the image intensifier output, capturing the response over a complete modulation period. Deficiencies in our measured response are clearly identifiable and simple modifications to the configuration of our electrical driver circuit improve the modulation performance.

***Index Terms*—Image intensifier, optical distance measurement, optoelectronic devices.**

I. Introduction

MEASURING the distance to an object is an important requirement for a number of applications including fields such as industrial inspection, surveying, and medical imaging. Various methods have been developed to acquire range measurements; however, each configuration also experiences a number of associated advantages and drawbacks. Typical systems such as stereo techniques suffer from reduced precision at extended distances and occlusion problems, and laser scanners tend to be slow due to the time required to serially scan a large area by mechanical means. A relatively new field involves using time-of-flight (either directly or indirectly) to measure range simultaneously over the entire field of view [1]–[9]. The parallel nature of this approach has the ability to produce high resolution images with short acquisition time.

Direct time-of-flight systems [1]–[3] emit a short light pulse, illuminating the entire field of view, which is reflected from objects within the scene. A complex receiver array is used to precisely measure the time delay of the reflection for each pixel within the array. The speed of light results in a short flight time for small distances, e.g., measuring an object with centimeter range precision necessitate resolving the flight time with $\sim$70 ps resolution. Extremely high-speed electronics are required in order to generate a fast rising edge to allow the flight time to be measured with this high level of precision. High sensitivity is also required to image objects that have low reflectivity, or are at a large distance from the receiver as the intensity of the returned signal is low. Avalanche photodiodes and digital counters operating at gigahertz (GHz) frequencies are typical components utilized in such a design. The complexity of the receiver limits the attainable pixel density, with typical arrays achieving 32×32 pixels [3].

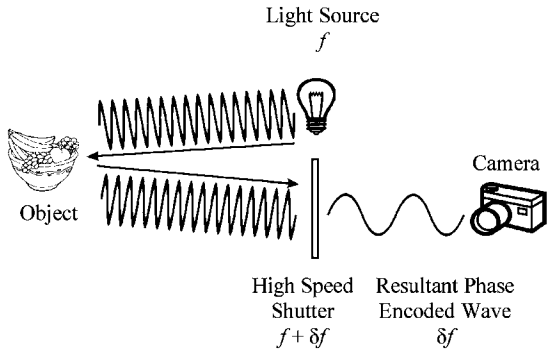

Fig. 1. Heterodyning range imager configuration.

Indirect time-of-flight measurement can significantly reduce the receiver (and emitter) complexity and bandwidth requirements, which in turn reduces system costs and often allows for a larger number of pixels within the detector array [4]–[10]. Our system uses a heterodyne technique where a light source is amplitude modulated, illuminating the entire field of view. The light is reflected from objects within the scene, imposing a phase shift in the received modulation envelope proportional to the object distance. A receiver, in this instance an image intensifier, is gain modulated at a frequency slightly different to that of the light source. The receiver acts as a mixer, producing a low-frequency beat signal at the output, as illustrated in Fig. 1. The phase shift in the illumination modulation envelope is preserved during the mixing process; hence the object range is encoded into the phase of the low-frequency beat signal.

By selecting a beat frequency of the order of a few hertz, the output from the image intensifier can be digitized with a conventional charge coupled device (CCD) video camera. From a minimum of three image frames, assuming sinusoidal oscillation, the recorded intensity values allow the beat signal phase to

Manuscript received October 01, 2007; revised February 28, 2008; accepted March 12, 2008. Current version published October 22, 2008. A. D. Payne acknowledges the support of TEC for providing a Top Achiever Doctoral Scholarship. The associate editor coordinating the review of this paper and approving it for publication was Dr. Dwight Woolard.

A. D. Payne, A. A. Dorrington, and M. J. Cree are with the University of Waikato, Hamilton 3240, New Zealand (e-mail: adp2@waikato.ac.nz; adrian@waikato.ac.nz; cree@waikato.ac.nz).

D. A. Carnegie is with the School of Chemical and Physical Sciences, Victoria University of Wellington, Wellington 6140, New Zealand (e-mail: dale.carnegie@vuw.ac.nz).

Digital Object Identifier 10.1109/JSEN.2008.2004577

be measured independently for each individual pixel. Finally, the distance d to each pixel is determined from the phase φ using (1), where c is the speed of light and f_m is the modulation frequency

$$d = \frac{c\varphi}{4\pi f_m}. \tag{1}$$

The precision σ of the range measurement for an amplitude modulated range finder is given as [11]

$$\sigma = \frac{c}{4\pi f_m m\sqrt{\mathrm{SNR}}} \tag{2}$$

where the additional terms m and SNR are the modulation index and signal-to-noise ratio, respectively. The modulation index (or depth) of a sinusoidal wave is the ratio of the peak-to-peak amplitude relative to the maximum peak value, with a range between zero and one. In the heterodyne imaging system, it is the product of the modulation index of the illumination source and image intensifier modulation waveforms. The signal-to-noise ratio term is used to encompass the entire system, and is determined not only by the components used to construct the imaging system, but also scene dependent parameters such as distance and surface scattering properties. To produce range images with high precision, it is clearly desirable to maximize the terms f_m, m and SNR wherever possible.

II. Image Intensifier

The operating principles of an image intensifier are well known [12], [13]. An image is focused on to an input window coated with a suitable photocathode material. When struck by a photon an electron is released, due to the material's low work function, which is accelerated by an applied electric field. The electron enters a microchannel plate (MCP) where collisions with the MCP walls emit secondary electrons, producing a multiplication effect of many orders of magnitude. Upon exiting the MCP, the electrons are again accelerated by an electric field, this time colliding with a phosphor screen, creating an output image. The "shutter" function is typically produced by varying the electric field at the photocathode. By applying a negative voltage (relative to the MCP), electrons are accelerated towards the MCP and an output image is formed, whereas a positive voltage deflects the electrons away from the MCP and turns the intensifier off.

Despite a number of well known drawbacks, image intensifiers are commonly used as high-speed shutters because they are generally the only practical off-the-shelf solution capable of operating at frequencies in excess of 100 MHz. The drawbacks include; requiring high voltage power supplies, reduction in image quality, highly nonlinear photocathode drive voltage to optical responsivity transfer function, and suffering from an irising effect when modulated at high frequencies. By characterizing the image intensifier's electronic and optical response in the range imaging system, some of these drawbacks can be mitigated by optimizing the operating conditions, thereby enhancing the range measurement precision.

The static image intensifier optical response can easily be measured by applying a uniform light source to the input window, while a DC voltage is applied to the photocathode.

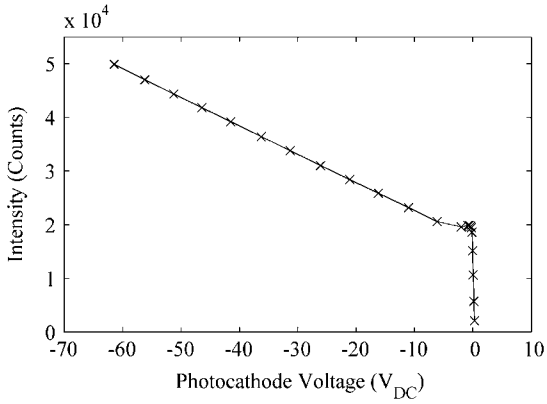

Fig. 2. Image intensifier DC optical gain for a range of photocathode input voltages.

The output intensity is measured with a CCD, while the voltage is slowly varied. As can be seen in Fig. 2, for a positive photocathode voltage the output drops to zero (slightly above zero in the graph due to CCD dark current). When the voltage becomes slightly negative, a large increase in gain occurs as the electrons emitted from the photocathode are accelerated towards the MCP. From about -2 V onwards, enhancing the electric field applied between the photocathode and the MCP increases the kinetic energy of each electron, increasing the image intensifier gain.

Producing a sinusoidal beat waveform as depicted in Fig. 1 is difficult due to the nonlinearity of the image intensifier photocathode voltage response. A near linear response can be achieved by restricting the photocathode voltage range, operating exclusively either above or below the "knee" in Fig. 2. For small voltages, the SNR is reduced due to the lower gain at the MCP. The photocathode voltage is also partially responsible for focusing the image onto the MCP, so the image resolution significantly deteriorates when small voltages are used [13]. In contrast, exclusively using larger negative voltages reduces the modulation index of the produced sine wave as the peak on/off gain ratio is less than 10 (image intensifiers are typically capable of generating an on/off ratio of 10^6 [12]). Neither case is acceptable as the measurement precision will be constrained according to (2).

For gated applications, where the image intensifier is pulsed on for a brief period, a photocathode voltage spanning the range -200 V to $+50$ V is typically used. In this instance, the parameter of interest is typically the pulse full width half maximum (FWHM), not the waveform shape. A similar voltage regime can be used for continuous modulation—at the expense of creating a distorted waveform shape containing harmonics. This has two effects for the range imaging system. First, the modulation index m of the nonsinusoidal waveform can exceed the maximum value of 1, which is beneficial as it improves the measurement precision using the relationship given in (2). Secondly, if the modulated illumination waveform also contains harmonics, then the harmonics produced propagate to the low frequency beat output signal. The beat signal must be sampled above the Nyquist rate to avoid aliasing; therefore a larger number of image frames must be captured compared with

the use of a sinusoidal modulation waveform. The capture of additional image frames increases the required acquisition time of the system, hence a tradeoff exists where nonsinusoidal modulation can be used to provide enhanced precision at the expense of operating speed. We selected this latter option during the design of our system.

Applying the full photocathode voltage range used in single pulse, gated applications (250 V_{pp}) to applications requiring continuous modulation at high frequencies is an unrealistic requirement due to both the difficultly of designing a practical electronic drive circuit, and also due to the corresponding power dissipation within the image intensifier. The photocathode, although primarily seen as a capacitive load, has a small resistance across its surface. When modulated with high frequencies and voltages, the resistance causes heating of the photocathode, potentially damaging the device.

For our application, a driver circuit was designed to operate over a smaller voltage range, providing an output of 50 V_{pp} at frequencies up to 100 MHz [14]. The circuit generates a square waveform with a rise and fall time of approximately 3.5 ns. To maximize the modulation index value the voltage should span the "knee" in Fig. 2, operating from a positive voltage to a negative voltage, while a large negative voltage is required to maximize the gain and spatial resolution [13]. A DC bias voltage is added to the MCP input to generate a relative voltage range of -40 V (on) to $+10$ V (off) as a compromise between these two constraints. Although a larger negative voltage is desirable, the relative per-voltage increase in spatial resolution and gain is minimal beyond -40 V [13].

Photocathode electrodes typically consist of a metal ring around the outer edge of the photocathode, to provide a low resistance path at the edge of the imaging area, while the photocathode material results in a larger resistance at the center. This resistance and the capacitance between the photocathode and the MCP limit the rate at which the drive voltage reaches the center of the photocathode. At high modulation frequencies, a well known "irising" effect can occur where the center of the image intensifier gating is delayed relative to the outer edge [15]. In our range imager application, this causes a flat object to appear curved, and more distant in the center [16].

III. Characterization

To ascertain the minimum number of captured image frames required to avoid aliasing requires knowledge of the harmonic content of the low frequency beat signal. Harmonics in the beat signal result from harmonics within the high-frequency illumination and image intensifier modulation waveforms. The illumination waveform can be measured with a photodiode and oscilloscope. The image intensifier modulation waveform can be approximately determined by measuring the electrical radio frequency (RF) photocathode voltage, and applying it to the DC image intensifier photocathode voltage response from Fig. 2. This approach is fairly limited as it cannot take into account spatial variations over the image intensifier (including irising), and assumes an identical static and dynamic image intensifier response. Care must be taken to ensure that the load seen by the driver circuit does not change during this measurement as the capacitive loading from a typical high impedance oscilloscope probe (10–15 pF) would alter the waveform significantly (our photocathode capacitance is approximately 60 pF). An optical method of measuring the image intensifier response is therefore preferable to avoid these issues.

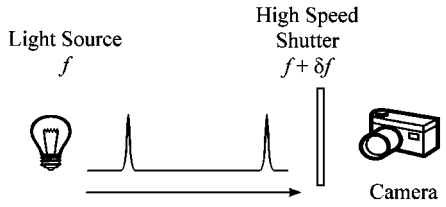

Fig. 3. Characterization configuration. A pulsed laser source with repetition rate f replaces the sinusoidal light source in the ranger configuration.

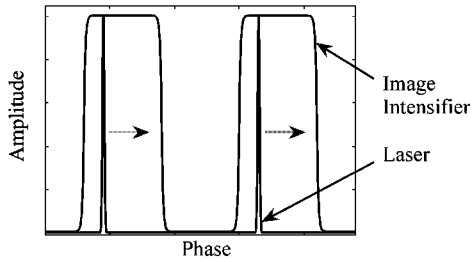

Fig. 4. The image intensifier is illuminated with a picosecond pulsed laser which samples the response at one point in the waveform. The relative phase of the laser pulse is continuously advanced, slowly scanning across the entire image intensifier waveform.

To optically measure the response, the range imaging system was modified, as shown in Fig. 3. A picosecond pulsed laser replaces the sinusoidal (or square) modulated light source, and illuminates the input window of the image intensifier. The short light pulse is used to temporally probe the intensifier gain at one instant in the modulation cycle, as illustrated in Fig. 4. The pulsed laser and the photocathode modulation electronics are both triggered from a digital synthesizer which generates two frequencies with a small frequency offset, creating a continuous relative phase shift between the laser pulse and the intensifier gating waveforms. This phase shift is designated by the right facing arrow in Fig. 4, indicating the continuous shift over time that the laser pulse experiences relative to the image intensifier waveform. To achieve a high SNR, a laser pulse is generated for every period of the image intensifier modulation, and the output is integrated at the CCD over a large number $(\sim 10^5)$ of pulses. The signal generator also provides a third output which is used to trigger the CCD, allowing it to be synchronized with the continuously changing phase offset, capturing a predetermined number of samples over the modulation waveform period.

A similar technique has been used to characterize the gated (pulsed) response of an image intensifier where a discrete electrical delay generator [15], [17], or an optical delay [18], is used to step the laser pulse over the image intensifier gain profile in a similar fashion to that shown in Fig. 4. Adjusting discrete-time delays is a cumbersome process, especially if it requires altering the optical path length to create the change in delay.

A distinction between our heterodyne method, and previous methods described, is that each sample that is acquired is separated by a phase offset, rather than a time delay. This difference between a phase offset and a time delay is significant for

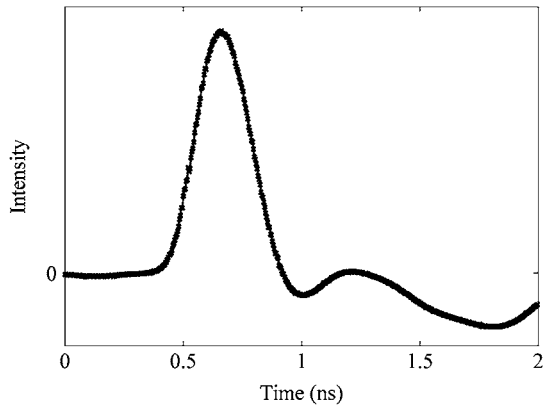

Fig. 5. Generated laser pulse, FWHM 266 ps.

systems where the modulation frequency f can be altered. By maintaining a constant frequency difference δf, the rate of the continuous phase change also remains constant. This allows the same number of samples to be collected over the modulation period regardless of the modulation frequency used.

IV. Laser Pulser

Laser pulser systems are readily available from a number of manufacturers; however, the requirements of this configuration make it relatively simple to construct a basic pulser circuit capable of low-frequency (less than 100 MHz) repetition rates. Only the pulse width is significant for this experiment as the MCP provides a large gain and, therefore, high peak optical power is not necessary.

Gain switching a laser diode produces a short optical pulse, down to tens of picoseconds, from a longer electrical pulse [19]. Carriers (electrons) are injected into the active region of the laser, bringing the number of carriers above the lasing threshold. Once above the threshold a large number of photons are produced by stimulated emission within the laser, which in turn reduces the number of available carriers back below the lasing threshold. If the current injected into the laser is turned off at this point, a short optical pulse is generated. A circuit was constructed to generate short pulses using this technique. A comparator first converts the sinusoidal output from the frequency synthesizer into a CMOS level square wave. The signal passes to two inputs of a CMOS AND gate, although one input is first past through an inverter logic gate. When the comparator toggles from low to high, both inputs to the AND gate are high for a duration matching the propagation delay of the inverter (approximately 3 ns), hence, a pulse is produced at the output. An iC-HK laser switch (iC-Haus GmbH, Bodenheim, Germany) is used to provide the pulsed current to the laser diode, and allows the peak current level to be adjusted to optimize the generated output pulse.

A recorded pulse is shown in Fig. 5 using a Hitachi HL6501MG laser diode. The FWHM pulse width of 266 ps shown is limited by the $\sim$2 GHz bandwidth of the photodiode used (SV2-FC, Thorlabs, NJ, USA), therefore the laser pulse may be shorter than that shown. Note that in Fig. 5 the pulse tail traverses below zero. This is an artifact of the photodiode impulse response caused by electrical ringing and is not part of the true optical pulse. For the purpose of this experiment, the pulse width shown is considered satisfactory as it is significantly shorter than the modulation period of the image intensifier.

V. Experimental Configuration and Results

The pulsed laser beam is expanded, and to minimize geometric variation across the face of the image intensifier, is placed approximately 1.5 m from the input window. Ground glass is placed in front of the image intensifier to ensure homogeneous illumination by partially diffusing the light to remove interference patterns generated by the laser. Under normal range finder operation a lens is used to focus the scene on to the image intensifier, but is removed during this experiment.

A direct digital synthesizer [14] produces the modulation signals for the image intensifier driver and the laser pulser at a selected frequency with a 0.1 Hz difference, hence it takes 10 s for the phase between the laser pulse and the image intensifier modulation signal to cycle through 360°. This differs from normal operation in the range imager configuration, where a 1 Hz (or higher) frequency difference is used to decrease the required acquisition time for each range measurement. Digital synthesizers can generate deterministic jitter when producing a square wave output due to discrete spurious frequency components contaminating the sinusoidal output [20]; to minimize this jitter attention must be paid to the reconstruction filter used. The synthesizer used is configured for wideband use with a low-pass filter below the Nyquist frequency, so an additional filter (BLP series, Mini-Circuits, NY, USA) is added at the appropriate cut off frequency for each test to remove additional harmonics. The output of the image intensifier is imaged onto a CCD digital video camera (Pantera TF 1M60, DALSA, Waterloo, Canada), that is configured to operate at 100 fps with an integration time of 8.2 ms. The 0.1 Hz frequency difference (δf) and 100 fps camera frame rate equates to capture of 1000 points over the image intensifier modulation period.

The exact number of pulses being integrated during each captured frame is a function of the modulation frequency being characterized, e.g., for a modulation frequency of 10 MHz, with a camera integration time of 8.2 ms, approximately 82 000 pulses are integrated during each frame, providing a high SNR.

A. Temporal Response

To measure the "shutter" action of the image intensifier, 49 pixels (7×7) in the center of the recorded image are averaged together (to further increase the SNR). A plot of the resulting optical gain of the image intensifier is shown in Fig. 6 for a modulation frequency of 10 MHz. The response is clearly far from desired, with significant ringing occurring due to the photocathode capacitance and the inductance of the interconnecting wires to the electronic driver forming an electrical resonant circuit. During the "on" state, the amplitude varies by up to 60%, and during the "off" state, the electrical ringing peak is large enough to bias the image intensifier on for short pulses. The nonzero minimum value is due to CCD dark current.

To improve the response, two modifications were carried out. The existing system coupled the modulation driver circuit output to a PCB which injected additional DC voltages required to bias the various stages within the image intensifier.

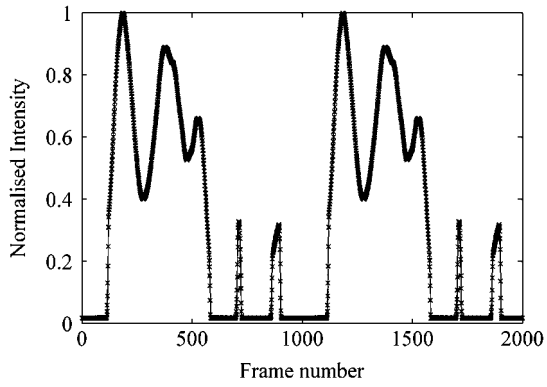

Fig. 6. Image intensifier response at a modulation frequency of 10 MHz. Additional peaks are caused by electrical ringing during the "off" period.

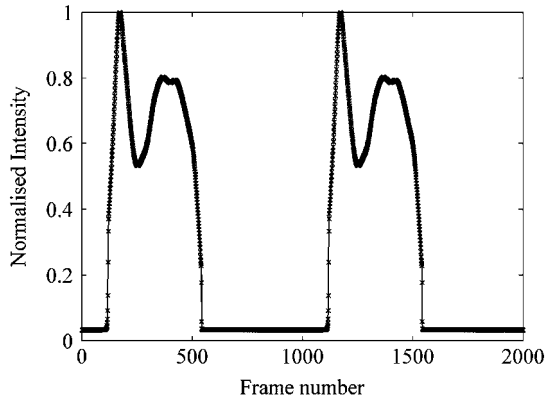

Fig. 7. Improved intensifier response at 10 MHz after redesigning the driver circuit and adjusting the bias voltage level.

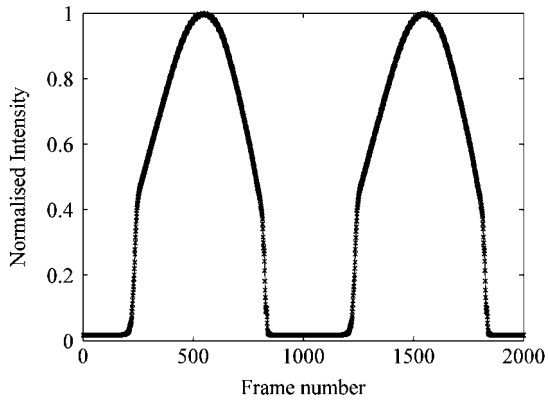

Fig. 8. Image intensifier response at 80 MHz.

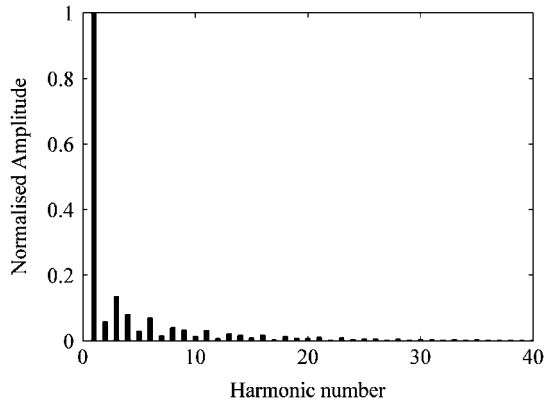

Fig. 9. A FFT of the data from Fig. 8 showing the spectrum of the image intensifier modulation waveform when operated at a frequency of 80 MHz.

This PCB was, in turn, connected to the image intensifier. To reduce the inductance of the interconnections and, therefore, the amplitude of the electrical ringing (hence optical ringing in Fig. 6), the RF amplifier circuit was redesigned to incorporate the required bias voltages without the need for the intermediate PCB. The interconnecting wires from the image intensifier were also reduced in length to further reduce inductance. The second modification was to simply adjust the bias voltages so that the ringing after the (optical) falling edge is unable to bias the intensifier on, corresponding to use of a modulation voltage between -38 V (on) to $+12$ V (off). The new response at the same 10 MHz modulation frequency is shown in Fig. 7. Significant improvement can be seen; ringing on the falling edge no longer causes the image intensifier to be biased on, and the ringing on the rising edge, although still large, has been reduced by 20%. Impedance matching the (low impedance) amplifier output to the image intensifier could potentially be used to further reduce this ringing if necessary. The electrical resonant frequency of the driver circuit and capacitive photocathode load can be estimated by the period of the observed ringing, and in this case is approximately 65 MHz.

It is desirable to modulate the image intensifier at a frequency higher than 10 MHz as the range measurement precision is proportional to the modulation frequency. The image intensifier driver circuit is designed to operate at frequencies up to 100 MHz, although due to increased power consumption when operating at higher frequencies, the power supply is unable to maintain regulation over the entire modulation frequency range. The maximum stable operating frequency was found to be limited to approximately 80 MHz, although a replacement power supply will extend this limit in the near future.

The characterization experiment was repeated at the 80 MHz modulation frequency; again capturing 1000 points over the modulation period by using a frequency difference δf of 0.1 Hz and a camera frame rate of 100 fps. The response is shown in Fig. 8. Operating above the electrical resonant frequency, ringing no longer causes significant degradation of the waveform shape. The harmonic spectrum of the response is determined by performing a fast Fourier transform (FFT) on the 80 MHz data, with the magnitude plotted in Fig. 9.

As previously mentioned, during normal range finder operation if the illumination waveform also contains harmonics, these harmonics can propagate to the low-frequency beat signal. Adequate sampling of the beat signal must be ensured to avoid aliasing. The phase of the fundamental frequency component is used to determine the object range; hence, contamination from aliasing occurs for frequencies with a harmonic number of i. $f_{\mathrm{samp}} \pm f_{\mathrm{sig}}$, where i is an integer, f_{samp} is the camera sampling rate, and f_{sig} is the beat frequency. Typically, during normal operation, the beat frequency δf is set to 1 Hz, and the camera is set to 29 fps [9]. From Fig. 9, it can be seen that the key candidates for contaminating the range measurement (with

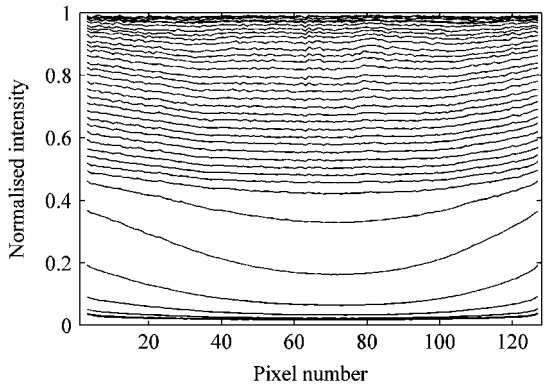

Fig. 10. Irising during rising edge at 80 MHz. Each ascending line spans the width of the image intensifier, and occurs at a delayed phase shift (equivalent to a time delay of 125 ps).

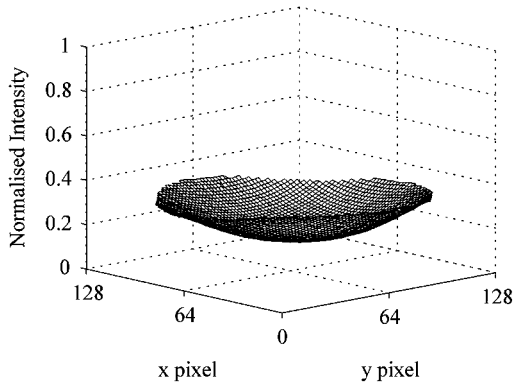

Fig. 11. Irising during the rising edge at 80 MHz. The gain at the center of the image intensifier is delayed due to photocathode resistance and capacitance.

harmonic numbers of 28 and 30) have negligible amplitude, hence the signal is considered to be adequately sampled, and aliasing concerns are avoided.

B. Spatial Response

The captured data can also be used to characterize the spatial response of the image intensifier during high-frequency modulation. It is expected that "irising" occurs due to the delay experienced by the changing voltage towards the center of the photocathode.

Approximating the image area by assuming it is symmetrical, the intensity of a row of pixels through the center of the image is plotted for a selection of captured frames. Fig. 10 shows the output intensity changing during the rise time, where each line plot is phase delayed (equivalent to a time delay of 125 ps). Significant irising can be seen to occur during a 500 ps interval where the lines are separated by large spacing (indicating a rapid change). The subsequent 3.5 ns illustrate a much slower change in intensity, and as such the irising is much less noticeable (although still present). From this figure, the electrical time delay from the edge to the center of the image is estimated to be 150 ps. The falling edge of the same 80 MHz frequency waveform exhibits similar levels of irising to that during the rising edge.

A 3-D plot of the normalized intensity of a single captured frame is shown in Fig. 11, again illustrating the irising over the entire image. The frame was selected from the rapid (rising) transition region where irising is most pronounced. The resulting image clearly shows the expected bowl shape rather than a flat surface, with reduced intensity near the center pixels compared with those at the outer edges. Note that the data have been spatially subsampled for clarity of the mesh.

For the estimated delay of 150 ps, range measurements will be elongated by $\sim$20 mm near the center relative to the outer edges, calculated using (3), where ΔL is the change in distance, c is the speed of light, and ΔT is the time delay. This value is in close agreement to residuals from experimental calibration of a known target [16]. This systematic error is an order of magnitude larger than the other errors in the system [9], and therefore has priority for calibration. As it is due to the physical construction of the image intensifier used, it is not possible to prevent it from occurring. Typical approaches to minimize irising are to use a smaller diameter image intensifier or to apply a conductive coating to the photocathode. Our image intensifier is designed to have a short gating time, hence already incorporates such a conductive coating. Replacing our 25 mm diameter image intensifier with a smaller device (e.g., 18 mm diameter) is a viable option, but comes at the expense of lower image quality and still does not completely eliminate the irising problem. For our application, the preferred solution is, therefore, to apply a correction to the range data during software processing

$$\Delta L = \frac{c.\Delta T}{2}. \tag{3}$$

VI. Discussion

Using the method introduced here, the number of samples taken over a waveform period is dependent on the camera frame rate and the difference in modulation frequencies, and is independent of the absolute modulation frequency of interest. This makes it trivial to acquire data over a large range of operating frequencies, in this case showing captures at 10 and 80 MHz each capturing 1000 samples per period. The maximum modulation frequency that can be accurately characterized is limited by the pulse width of the laser, although this can be extended to some extent if the laser pulse shape is measured with a high-speed photodiode and a deconvolution performed on the captured data sequence to recover the true image intensifier response.

The image intensifier response clearly showed undesirable oscillation and superfluous peaks, which are obscured by the extended light pulse width during normal operation of the range finder. The minor alterations made to the electrical configuration, adjusting the MCP voltage and modifying the physical connection, completely removed the unwanted peaks and reduced the oscillation amplitude.

The oscillation is due to the undesirable resonant electrical circuit formed between the photocathode capacitance and inductance at the RF amplifier output and interconnecting wires. The circuit has an associated electrical resonant frequency that can be determined from the period of the oscillation during the turn-on transition while operating the system at a low frequency (1 to 10 MHz). Knowledge of this frequency allows us to select a suitable frequency range at which to operate the range imager

with minimal waveform distortion occurring. The selected modulation frequency should ideally be as high as possible to maximize the range measurement precision, although the bandwidth and power dissipation of the image intensifier driver circuit constrain the upper frequency limit achievable. The graphs shown for an 80 MHz response indicate that the image intensifier temporal response in this frequency range is close to ideal.

The electrical waveform applied to the image intensifier ranges from $+12$ V (off) to -38 V (on) to maximize the modulation index, gain, and spatial resolution. A side effect of this asymmetry around 0 V occurs during high-frequency operation, where the duty cycle of the image intensifier response increases due to the limited driver circuit bandwidth (as the electrical waveform can no longer be considered square). The characterization method shown here provides a means for measuring this change over the modulation frequency range of interest. In the range imager application, an increase of the image intensifier duty cycle reduces the available CCD dynamic range for measuring the low frequency beat signal. The reduction is apparent when the light source and image intensifier signals are 180° out of phase; if the duty cycle is greater than 50%, the two signals will still partially overlap and, therefore, it is not possible to produce a "black" output at the CCD. Reduction of the dynamic range increases susceptibility to noise in the phase measurement. To compensate for this effect, the duty cycle of the electrical waveform was intentionally reduced to approximately 40%. At the lower operating frequency of 10 MHz this reduced duty cycle is clearly visible in the optical response (Fig. 7), while at 80 MHz, Fig. 8, the duty cycle increases as expected. Ideally the electrical duty cycle would be reduced further; however, it is constrained by the bandwidth of the driver circuit.

A number of "lock-in pixel" or "demodulation pixel" arrays are being developed by various groups [4], [7], [10], that synchronously detect modulated light directly with CCD or CMOS technologies in a similar manner to that used by the range imaging system described here. This removes the requirement of using an image intensifier, and therefore its associated disadvantages, but is typically limited to operating at frequencies below 20 MHz, and with low image resolutions. Multitap solutions, which simultaneously collect two or four samples at different phase angles, can suffer from problems with matching the gain and duty cycle applied to each tap. The characterization technique shown here is directly applicable to these sensors, and could be used to help optimize and match each tap response.

VII. Conclusion

An image intensifier is used as a modulated optical shutter in a full field range imaging system. The ranging system uses a heterodyne configuration to generate a low-frequency beat signal from a high-frequency modulated illumination source and modulated optical shutter. The low-frequency beat signal is captured by a CCD camera, and the phase of each pixel, which is proportional to the distance of each object, is calculated from the captured image sequence.

To optimize the range measurement precision and accuracy, the image intensifier was characterized to investigate and optimize its temporal and spatial response. In this application, the range measurement precision is dependent on the modulation frequency, the modulation index (or depth), and the SNR; therefore, the image intensifier was configured to maximize these parameters where possible. The experiments revealed that the optical response deviated from the ideal response, most notably with electrical ringing causing a number of problems for low-frequency (< 50 MHz) operation. This ringing emphasizes the fact that the response is dependent on both the image intensifier and the electronic driver as a complete system, and as such simple modifications to the electronic driver improved the optical response.

The optical modulation waveform shape is also an important factor in this application, as harmonics can propagate to the low-frequency beat signal. These harmonics can be aliased during sampling, contaminating the phase (hence range) measurement. By measuring the image intensifier modulation waveform shape and performing a FFT, the harmonic content can be determined, and the minimum required CCD sampling rate established to avoid aliasing.

Spatial characterization of the intensifier gain showed irising, where modulation at the center of the image is delayed relative to the outer edge. It is an inevitable consequence of image intensifier technology, and distorts the range measurement, with objects at the center of the image appearing to be at a greater distance than those at the outer edges. Postprocessing is required to correct for this effect and the results from the spatial characterization can be used to generate the required correction for each modulation frequency.

Past operation of the full-field range imaging system has demonstrated measurement precision of less than 1 mm out to 5 m range [9]; the characterization and resulting modifications discussed here are expected to further enhance this precision.

References

[1] H. Ailisto, V. Heikkinen, R. Mitikka, R. Myllyla, J. Kostamovaara, A. Mantyniemi, and M. Koskinen, "Scannerless imaging pulsed-laser range finding," *J. Optics A—Pure and Applied Optics*, vol. 4, pp. S337–S346, 2002.

[2] M. A. Albota, R. M. Heinrichs, D. G. Kocher, D. G. Fouche, B. E. Player, M. E. O'Brien, B. F. Aull, J. J. Zayhowski, J. Mooney, B. C. Willard, and R. R. Carlson, "Three-dimensional imaging laser radar with a photon-counting avalanche photodiode array and microchip laser," *Appl. Opt.*, vol. 41, pp. 7671–7678, 2002.

[3] C. Niclass, A. Rochas, P. A. Besse, and E. Charbon, "Design and characterization of a CMOS 3-D image sensor based on single photon avalanche diodes," *IEEE J. Solid-State Circuits*, vol. 40, pp. 1847–1854, 2005.

[4] T. Oggier, "SwissRanger SR3000 and first experiences based on miniaturized 3D-TOF cameras," *Proc. 1st Range Imaging Research Day*, pp. 97–108, 2005.

[5] M. Kawakita, K. Iizuka, H. Nakamura, I. Mizuno, T. Kurita, T. Aida, Y. Yamanouchi, H. Mitsumine, T. Fukaya, H. Kikuchi, and F. Sato, "High-definition real-time depth-mapping TV camera: HDTV axi-vision camera," *Opt. Express*, vol. 12, pp. 2781–2794, 2004.

[6] A. Medina, F. Gaya, and F. del Pozo, "Compact laser radar and three-dimensional camera," *J. Opt. Soc. Amer. A*, vol. 23, pp. 800–805, 2006.

[7] S. B. Gokturk, H. Yalcin, and C. Bamji, "A time-of-flight depth sensor—System description, issues and solutions," in *Proc. 2004 IEEE Conf. Comput. Vision Pattern Recogn. Workshop*, 2004, p. 35.

[8] R. O. Nellums, R. D. Habbit, M. R. Heying, T. A. Pitts, and J. V. Sandusky, "3D scannerless ladar for orbiter inspection," in *Proc. SPIE—Spaceborne Sensors III*, 2006, vol. 6220, p. 62200G.

[9] A. A. Dorrington, M. J. Cree, A. D. Payne, R. M. Conroy, and D. A. Carnegie, "Achieving sub-millimeter precision with a solid-state full-field heterodyning range imaging camera," *Meas. Sci. Technol.*, vol. 18, pp. 2809–2816, 2007.

[10] R. Schwarte, "Breakthrough in multichannel laser-radar technology providing thousands of high-sensitive lidar receivers on a chip," in *Proc. SPIE*, 2004, vol. 5575, pp. 126–136.
[11] A. Jelalian, *Laser Radar Systems*. Norwood, MA: Artech House, 1992.
[12] L. J. van Vliet, F. R. Boddeke, D. Sudar, and I. T. Young, "Image Detectors for Digital Image Microscopy," in *Digital Image Analysis of Microbes: Imaging, Morphometry, Fluorometry and Motility Techniques and Applications*, M. H. F. Wilkinson and F. Schut, Eds. Chichester, U.K.: Wiley, 1998, pp. 17–25.
[13] L. A. Bosch, "Dynamic uses of image intensifiers," in *Proc. SPIE Photoelectronic Detectors, Cameras, and Systems*, 1995, vol. 2551, pp. 159–172.
[14] A. D. Payne, D. A. Carnegie, A. A. Dorrington, and M. J. Cree, "Full field image ranger hardware," in *Proc. 3rd IEEE Int. Workshop on Electronic Design, Test and Applications (DELTA'06)*, 2006, pp. 263–268.
[15] P. Höß, K. Fleder, and J. Ehrhardt, "Subnanosecond optical gating using coax cable input microchannel plate image intensifier," *Opt. Eng.*, vol. 37, pp. 2213–2216, 1998.
[16] A. A. Dorrington, M. J. Cree, D. A. Carnegie, A. D. Payne, and R. M. Conroy, "Heterodyne range imaging as an alternative to photogrammetry," in *Proc. SPIE 6491—Videometrics IX*, San Jose, CA, 2007.
[17] M. Thomas, "Fast optical gating using planar-lead MCPIIS and linear microstrip impedance transformers," in *Proc. SPIE Int. Soc. Opt. Eng.*, 1994, vol. 2273, pp. 214–225.
[18] S. W. Thomas, A. R. Shimkunas, and P. E. Mauger, "Subnanosecond intensifier gating using heavy and mesh cathode underlays," in *Proc. SPIE, 19th Int. Congr. High-Speed Photography and Photonics*, 1991, vol. 1358, pp. 91–99.
[19] K. Y. Lau, "Short-Pulse and high-frequency signal generation in semiconductor-lasers," *J. Lightw. Technol.*, vol. 7, pp. 400–419, 1989.
[20] D. Brandon, AN-823 direct digital synthesizers in clocking applications time jitter in direct digital synthesizer-based clocking systems [Online]. Available: http://www.analog.com/UploadedFiles/Application_Notes/441653047757097406921314618 31AN823_0.pdf, accessed Apr. 2006

Andrew D. Payne received the B.Tech. and M.Sc. degrees from the University of Waikato, Hamilton, New Zealand, in 2003 and 2004, respectively. He is currently working towards the Ph.D. degree at the Department of Electronic Engineering, University of Waikato.

His research interests include mixed-signal (analogue, digital, RF) circuit design, embedded controllers, sensors, and optoelectronics.

Adrian A. Dorrington received the Ph.D. degree from the University of Waikato, Hamilton, New Zealand, in 2001.

He has held Postdoctoral Fellowships from the National Research Council (USA) at the NASA Langley Research Center, and from the Foundation for Research, Science, and Technology (New Zealand) at the University of Waikato. Currently, he is a Senior Lecturer in the Department of Engineering, University of Waikato. His research interests include optoelectronics and optical measurement technologies and, in particular, ranging, photogrammetry, and 3-D surface profiling.

Michael J. Cree (M'93–SM'05) is Senior Lecturer of Physics and Electronic Engineering at the University of Waikato, Hamilton, New Zealand. He has research interests in a variety of imaging applications including medical retinal imaging, hyperspectral imaging, gamma camera technology, and range imaging.

Dr. Cree is an active member of the Computer Vision Community in New Zealand and convened the Image and Vision Computing New Zealand Conferences in 2000 and 2007. He is a member of The Australasian College of Physical Scientists and Engineers in Medicine, and of the New Zealand Institute of Physics.

Dale A. Carnegie (M'91–SM'02) received the M.Sc. degree (First Class Honors) in physics and electronics and the Ph.D. degree in computer science from the University of Waikato, Hamilton, New Zealand.

He is currently a Reader in Electronic and Computer Systems Engineering at Victoria University of Wellington, New Zealand, where he heads the Mechatronics Research Group and coordinates the Computer Systems Engineering Program. His research interests are in the areas of autonomous mobile robotics, sensors, embedded controllers, and applied artificial intelligence.